Medical Hypotheses 131 (2019) 109315

Contents lists available at ScienceDirect

Medical Hypotheses

journal homepage: www.elsevier.com/locate/mehy

Is it possible to detect cerebral dominance via EEG signals by using deep learning?

Suat Toraman[a], Seda Arslan Tuncer[b], Ferhat Balgetir[c,*]

[a] Firat University, Department of Informatics, 23119 Elazig, Turkey
[b] Firat University, Department of Software Engineering, 23119 Elazig, Turkey
[c] Firat University, Faculty of Medicine, 23119 Elazig, Turkey

ARTICLE INFO

Keywords:
Electroencephalography
Speech center
Dominant hemisphere
Machine learning
Convolutional neural network
Classification

ABSTRACT

Each brain hemisphere is dominant for certain functions such as speech. The determination of speech laterality prior to surgery is of paramount importance for accurate risk prediction. In this study, we aimed to determine speech laterality via EEG signals by using noninvasive machine learning techniques. The retrospective study included 67 subjects aged 18–65 years who had no chronic diseases and were diagnosed as healthy based on EEG examination. The subjects comprised 35 right-hand dominant (speech center located in the left hemisphere) and 32 left-hand dominant individuals (speech center located in the right hemisphere). A spectrogram was created for each of the 18 EEG channels by using various Convolutional Neural Networks (CNN) architectures including VGG16, VGG19, ResNet, MobileNet, NasNet, and DenseNet. These architectures were used to extract features from the spectrograms. The extracted features were classified using Support Vector Machines (SVM) and the classification performances of the CNN models were evaluated using Area Under the Curve (AUC). Of all the CNN models used in the study, VGG16 had a higher AUC value (0.83 ± 0.05) in the determination of speech laterality compared to all other models. The present study is a pioneer investigation into the determination of speech laterality via EEG signals with machine learning techniques, which, to our knowledge, has never been reported in the literature. Moreover, the classification results obtained in the study are promising and lead the way for subsequent studies though not practically feasible.

Introduction

Brain is a complex organ primarily responsible for balance and decision-making processes. In particular, human brain is more complex compared to that of other living organisms. One of these complexities is known as 'cerebral dominance' which is defined as the relative superiority of one hemisphere over the other in the control of cerebral functions. In other words, it is the ability of one cerebral hemisphere to predominately control specific tasks [1]. Accordingly, damage to one of these hemispheres may result in the impairment of certain identifiable functions. For instance, damage to the left hemisphere can impair functions associated with speech, reading, and writing, whereas damage to the right hemisphere may result in a decreased ability to perform such tasks as judging distance, determining direction, and recognizing tones and similar artistic functions [2].

More than 90% of people worldwide are right-handed and the language-related functions are controlled by the left hemisphere in most of these individuals [1–3]. Fig. 1 illustrates the dominance of right and left hemispheres in the control of the left and right hands, respectively.

The brain consists of two hemispheres including right and left hemispheres and each hemisphere are divided into 4 lobes: frontal (F), parietal (P), temporal (T), and occipital (O) [5]. The term 'speech center' refers to two interconnected brain areas (Broca's and Wernicke's areas) that are associated with speech processing and production. Wernicke's area covers the middle two-thirds of the superior temporal gyrus and is associated with the interpretation of extrinsic (e.g. visual, auditory) and intrinsic (e.g. pain) senses. Broca's area is located in the posterior-inferior frontal gyrus and is the motor speech-production area where motor patterns are initiated for the expression of words and short phrases. The sensory information interpreted and synthesized through the signals received from Wernicke's area is transferred to Broca's area [6].

Literature reviews indicate that numerous studies have been conducted with various methods to provide a better understanding of the dynamic structure of the brain [7]. Of these, functional magnetic

* Corresponding author.
E-mail addresses: storaman@firat.edu.tr (S. Toraman), satuncer@firat.edu.tr (S.A. Tuncer), ferhatbalgetir@firat.edu.tr (F. Balgetir).

https://doi.org/10.1016/j.mehy.2019.109315
Received 11 June 2019; Received in revised form 13 July 2019; Accepted 19 July 2019

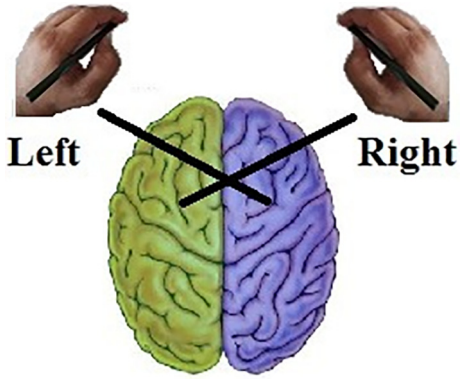

Fig. 1. Dominance of right and left hemispheres in the control of the left and right hand [4].

resonance imaging (fMRI) is a time-taking method and its results may be difficult to interpret. Additionally, intracarotid amobarbital procedure (Wada testing) is also used in the determination of the dominant hemisphere, although its use is limited due to its invasive nature and high risk of complications [8]. In the literature, there have been studies using MRI for the determination of speech laterality or the dominant hemisphere [9]. However, to our knowledge, these studies have provided inconclusive findings for the determination of the dominant hemisphere [10].

Electroencephalography (EEG) is a noninvasive, cost-effective diagnostic method which refers to the recording of the brain's spontaneous electrical activity over a short period of time and is commonly used in the diagnosis and treatment of epilepsy. EEG records reversible, irreversible, or progressive changes in the electrical activity of neurons in the presence of a focal or diffuse brain pathology or to rule out an organic pathology. As the EEG signals are nonlinear and dynamic in nature, they are highly complex and difficult to interpret by visual assessment [5]. Traditionally, neurologists perform direct visual inspection to identify epileptiform abnormalities. However, this technique can be time-consuming and may provide variable results based on the expertise level of the physicians. For these reasons, it is essential to develop a Computer-Aided Diagnosis (CAD) system to automatically identify the class of these EEG signals using machine learning techniques.

Deep learning is a machine learning technique based on representation learning, in which the system automatically learns and detects the features required for classification through processing of multiple layers of input data. This technique has been used in numerous computer-aided biomedical software programs [11,12].

In the present study, we propose the use of a CAD model for the determination of speech laterality. The model involves the use of deep learning techniques for the determination of speech laterality in both right- and left-hand dominant individuals without hand-designed feature extraction and selection.

To achieve this, the EEG signals of 67 subjects including both right- and left-hand dominant individuals were classified using 7 different CNN models, followed by the evaluation of classification performance for each model. In this way, a decision support system was established for the determination of speech laterality via EEG signals and also the performances of the CNN models in the classification of signals were compared with each other.

Materials and methods

Materials

The retrospective study included 67 subjects aged 18–65 years who had no chronic diseases and were diagnosed as healthy based on EEG examination in Firat University Hospital between January 2017 and January 2018. The subjects comprised 35 right-hand dominant (speech center in the left hemisphere) and 32 left-hand dominant individuals (speech center in the right hemisphere). The study was approved by (Non-Invasive Research Ethics Committee of Firat University) (Date: June 20, 2018; Approval No.: 269497).

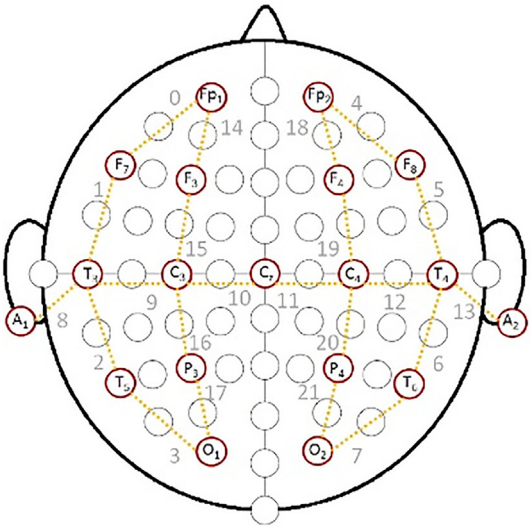

Fig. 2. Electrode placement according to the international 10–20 system [13].

The EEG data were retrieved from the 12-min EEG recordings performed for each subject by using a Nicolet EEG v32 device. The EEG data were recorded with 18 electrodes positioned on the scalp at FP1, FP2, F3, F4, C3, C4, P3, P4, O1, O2, F7, F8, T3, T4, T5, T6, A1, and A2, according to the International 10–20 system (Fig. 2) [13].

Methods

Speech laterality was determined in each subject via EEG signals. Spectrograms were created based on the EEG signals recorded from 18 channels and were later resized and used as the input to the CNN to be used for the establishment of a decision support system. Using the CNN models, a feature vector was extracted from each spectrogram to determine speech laterality and these vectors were classified with SVM. The classified data were compared with the diagnoses made by a specialist physician and were evaluated based on the performance criteria commonly used in the literature. Fig. 3 illustrates the decision support system employed in the study.

Creation of spectrograms

The Short-Time Fourier Transform (STFT) is a general-purpose tool for signal processing, providing information for both the time and frequency of a signal. In STFT, the Fourier transform is calculated by multiplying the transformation function with a window function. A spectrogram is a visual representation of the spectrum of frequencies of a signal as it varies with time. Spectrograms were created from the EEG signals to perform feature extraction with CNN models (Fig. 3) [14]. Spectrogram images were generated at MATLAB software. Data sets were trained using Python 3.6 and Keras 2.1.6 [15] on a computer with an Intel Core i3-2120 CPU (3.30 GHz).

Feature extraction with a pre-trained CNN model

CNN is a particular type of multi-layer sensors developed to mimic the physiology of the human visual system. CNN is commonly used in deep learning and has been shown to achieve empirical successes in tasks such as object recognition and signal processing and classification. The CNN architectures including VGG16, VGG19, ResNet, MobileNet, NasNet, and DenseNet201 were used to perform feature extraction from

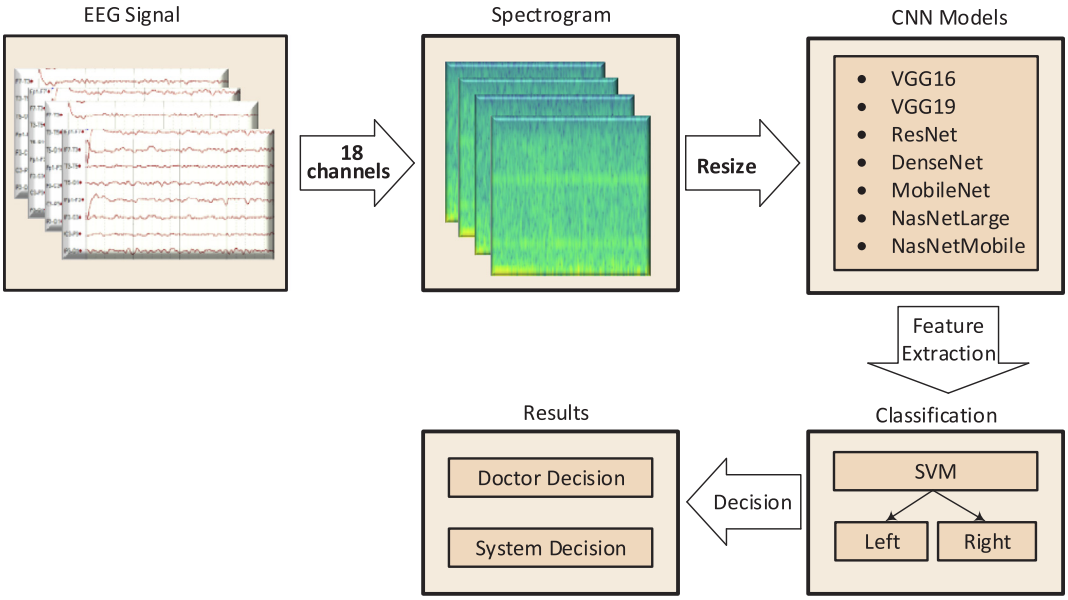

Fig. 3. Decision support system employed in the study.

the spectrograms created based on the EEG signals.

Large training data and computing power are needed to pre-train a CNN model for a specific task. In the lack of these opportunities, a transfer learning approach can be used, which is primarily used for creating a feature vector from a dataset in a different region of interest by using a CNN pre-trained for a specific task [16].

The input image dimension can vary across CNN models; while a 224 × 224 image input dimension is used in VGG16, VGG19, ResNet, DenseNet, MobileNet, and NasNetMobile, a 331 × 331 image input dimension is used in NasNetLarge. Therefore, each spectrogram in our study was resized according to the image input dimension of each CNN model. A feature vector was extracted from each CNN model by using the transfer learning method. Table 1 presents the dimensions of the feature vectors resized for each CNN model.

VGG16 and VGG19. The VGG models were invented by the Oxford University Visual Geometry Group (VGG). VGG16 uses small filters (3 × 3) rather than the large filters, as those used by AlexNet (11 × 11, 9 × 9). VGG16 consists of 13 convolution layers and 3 fully connected layers and also includes five max-pooling layers of size 2 × 2, with the final layer as the soft-max layer. VGG16 applies rectification nonlinearity (ReLu) activation and has approximately 138 million parameters. In contrast, VGG19 consists of 16 convolution layers and 3 fully connected layers and has approximately 144 million parameters [15,17].

Residual network (ResNet). As the depth of the network in CNN increases, the training becomes more difficult, ultimately leading to a problem known as 'vanishing gradients'. To overcome this problem, Residual Network (ResNet) has been developed, which arithmetically adds the input *(x)* to the *F(x)* to pass *(F(x) + x)* through Relu and also creates a shortcut path from the input *(x)* to the output to bypass multiple layers, instead of performing mapping with the nonlinear function *F(x)* in normal CNN. In this way, the training process is administered more easily. ResNet50 consists of 50 layers and has approximately 25.6 million parameters [18], implicating that ResNet50 has a lower number of parameters compared to the CNN models aforementioned. On the other hand, there are two other ResNet models including ResNet101 and ResNet152.

Table 1
Dimensions of feature vectors resized for each CNN model.

Model	Feature Size	Parameters
VGG16	4096	138 M
VGG19	4096	143.6 M
ResNet50	2048	25.6 M
DenseNet201	1920	20 M
MobileNet-V1	1024	4.2 M
NasNetMobile	1056	5.3 M
NasNetLarge	4032	89 M

Dense Convolutional network (DenseNet). Dense Convolutional Network (DenseNet) is a deep CNN model that connects each layer to every other layer in a feed-forward fashion. Though similar to ResNet in architecture, it has various differences. In ResNet, the feature-maps of all preceding layers are used as inputs, and the own feature-maps of each layer are used as inputs into all subsequent layers, in order to maximize the information flow between all the layers. Another major difference between ResNet and DenseNet is that ResNet does not concatenate feature-maps when extracting the input features of a layer, and instead uses all of the feature-maps from the previous layer as input to the subsequent layer [19].

MobileNet. MobileNet is a CNN architecture more suitable for mobile and embedded based vision applications where there is lack of compute power. In this architecture, depthwise separable convolutions which significantly reduce the size and complexity of the model are used to construct a light-weight deep CNN. Normally, the model size is the primary concern in the establishment of small networks. In MobileNet, however, the primary concern is the optimization of delay [20].

NasNet. Google researchers created an Automatic Machine Learning (AutoML) technique named Neural Architecture Search Network (NasNet) that can build a novel neural network using machine learning techniques (based on a certain dataset). The system transfers the best learned architecture on small datasets such as AutoML and CIFAR10 to large datasets such as ImageNet. NasNet has two distinct versions including NasNetLarge and NasNetMobile [21].

Classification of EEG signals

Support Vector Machines (SVM) is a machine-learning algorithm based on the structural risk minimization principle that is extensively

used for classification problems [22]. The primary goal of SVM is to find out the optimal hyper plane for the classification and employs its decision function to differentiate two classes. Eq. (1) demonstrates the decision function used in SVM classification:

$$f(x): sgn\left(\sum_{i=1}^{n} y_i \alpha_i K(x, x_i) + b\right) \quad (1)$$

In this equation, α_i indicates Lagrange multipliers, x_i indicates support vectors, and b indicates bias [23,24]. When linear discrimination is not applicable, the following kernel function can be used instead:

$$\text{Radial Basis Function (RBF): } K(x_i, x_j) = \exp\left(\frac{-||x_i - x_j||^2}{2\sigma^2}\right) \quad (2)$$

$$\text{Polynomial: } K(x_i, x_j) = (x_i x_j + 1)^d \quad (3)$$

Here, σ and d represent kernel parameters.

Performance evaluation

An objective performance evaluation of the CNN models used in the study was administered using k-fold cross-validation. A 10-fold cross validation was implemented and the dataset was divided into 10 folds, of which 9 folds were used for the training and the remaining one fold for testing. The same procedure was repeated for each part. Subsequently, the performance of each model was calculated as the average value of 10 folds. The classification performance of each model was evaluated based on the parameters including sensitivity, specificity, False Positive Rate (FPR), False Discovery Rate (FDR), F_1-score and AUC [25]. These parameters were defined using the Confusion Matrix shown in Fig. 4.

True-positive (TP): Number of left hemispheres identified correctly

False-negative (FN): Number of left hemispheres identified incorrectly

True-negative (TN): Number of right hemispheres identified correctly

False-positive (FP): Number of right hemispheres identified incorrectly

The sensitivity and specificity values were calculated using the following formulas:

$$Sensitivity = \frac{TP}{TP + FN} \times 100 \quad (4)$$

$$Specificity = \frac{TN}{TN + FP} \times 100 \quad (5)$$

$$Accuracy = \frac{TP + TN}{TP + TN + FP + FP} \quad (6)$$

$$False\ Positive\ Rate = \frac{FP}{FP + TN} \quad (7)$$

$$False\ Discovery\ Rate = \frac{FP}{FP + TP} \quad (8)$$

$$F_1\ Score = 2 * \frac{Precision * Recall}{Precision + Recall} \quad (9)$$

	Predicted (0)	Predicted (1)
Actual (0)	TN	FP
Actual (1)	FN	TP

Fig. 4. Confusion Matrix.

In clinical practice, laboratory parameters, clinical observations, and various diagnostic methods are commonly used to assess the wellbeing of individuals. By using these methods, a positive or negative diagnosis is made for each unit by comparing the measurement to the cutoff value. Receiver Operating Characteristic (ROC) is a graphical plot displaying sensitivity or True Positive Rate (TPR) as the y coordinate and the *1-specificity or FPR* as the *x* coordinate across a series of cutoff points. The area under the ROC curve is used as a scale for determining the superiority of a diagnostic procedure over the others. A higher AUC indicates a better overall diagnostic performance for test in the prediction of a disease [26,27]. Based on these facts, we also calculated AUC as a criteria for the performance evaluation of the models used in the study.

Results

A spectrogram was created for each EEG channel. Each spectrogram was calculated using a 48-ms Hamming window corresponding to 16 ms, with a 256-point fast Fourier transform and an image dimension of 875 × 656. Fig. 5a and b show the transformation of EEG signals into a spectrogram in a right-hand dominant and a left-hand dominant subject, respectively.

Since the image input dimension varies across CNN models, each spectrogram was resized as appropriate to each model. Table 1 presents the dimensions resized for each CNN model. A feature vector was constructed for each model and these feature vectors were used for SVM classification of EEG signals. In the classification, SVM was performed with different kernel functions including linear, Radial Basis Function (RBF), and polynomial along with a range of C values $[10^{-3}, 10^{+3}]$. Feature extraction was performed by using all the 18 channels of EEG signals as the input to CNN.

Table 2 presents the performance values obtained via SVM classification for each CNN model as well as the Sen (%), Spe (%), NPV (%), FPR (%), FDR (%), Acc (%), F_1 score (%) and AUC values for different kernel functions.

The classification results can be analyzed based on the specificity and sensitivity values. However, as these parameters do not provide information regarding the accuracy of the classification, they needed to be supported by ROC curve analysis and F1-score analysis. Receiver Operating Characteristic (ROC) analysis is commonly used to quantify how accurately a diagnostic test can discriminate between two states. The discriminatory power of the test increases as the ROC curve gets closer to the upper left corner. Moreover, a higher AUC indicates a better overall diagnostic performance for test. Considering that AUC indicates the predictive value of diagnostic tests, it was employed to evaluate the classification performance of the features extracted via each CNN model. It was revealed that VGG16 had the highest AUC value (0.83 ± 0.05). (Fig. 6a). Fig. 6 illustrates the ROC curves for each CNN model in the respective order presented in Table 2 and Fig. 6 presents the AUC values calculated for each CNN model based on the ROC curves.

Discussion

Speech laterality is typically determined using invasive methods such as intracarotid amobarbital procedure (Wada testing) or imaging techniques such as fMRI. However, to our knowledge, there has been no study in the literature reporting on the determination of speech laterality via EEG signals. In the present study, we aimed to determine speech laterality by using EEG signals with machine learning techniques. To this end, we employed various CNN models and also evaluated the performance of each model in the classification of EEG signals.

The structure of a spectrogram derived from EEG data differs markedly between right- and left-hand dominant individuals with atypical speech lateralization. As can be seen in the spectrograms of our subjects (Fig. 5), the frequency distribution of signals differs between

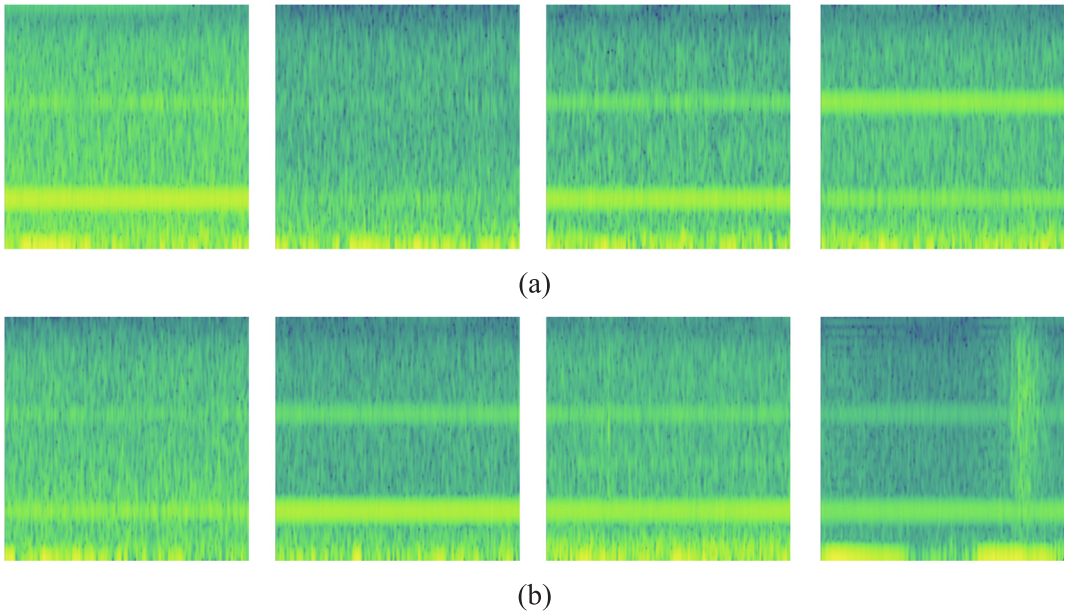

Fig. 5. (a) Spectrogram in a right-hand dominant subject, (b) Spectrogram in a left-hand dominant subject.

right and left-hand dominant individuals. However, although these differences are not discernible by naked eyes, they are represented in the frequency domain.

Feature extraction has a direct effect on the classification performance of CNN models. Accordingly, we employed several CNN models (VGG16, VGG19, ResNet, MobileNet, and NasNet) for feature extraction to obtain more reliable results. These models were administered for the extraction of both separate and concatenated features in all the 18 channels and each extracted feature was evaluated separately. Meaningfully, the higher classification performance achieved by the extraction of the features of all EEG signals indicates that the concatenated features have a higher representation power (Table 2).

In a study conducted in 1990, Wyllie et al. determined hemispheric dominance for language by using Wada testing and defined the speech-related regions in the dominant hemisphere as posterior temporal (Wernicke's area), frontal (Broca's area), and basal temporal regions [28]. Recent studies, however, have shown that aphasia may be present in other deep brain regions such as thalamus and thalamic lesions are associated with aphasia [29–31]. Based on these findings, it is tempting to consider that the speech center may not necessarily be localized in a specific region in the dominant hemisphere but rather can affect multiple regions including deep brain structures. This assumption, then, explains the remarkably high discriminatory ability of the CNN models in our study that employed the feature-maps obtained from all the channels used in EEG signals.

In our study, the SVM algorithm with appropriate parameters (learning environment, error of premature termination) was employed to provide an accurate classification of the features extracted via deep learning layers. The SVM parameters were combined with each other based on the characteristics of each CNN model. Moreover, different kernel functions were used for the classification, which further increased the success of the classification.

As seen in Table 1, both VGG16 and VGG19 have higher computational complexity compared to other deep CNN models [15]. In contrast, MobileNet and NasNetMobile are the models with the lowest computational complexity, which have been developed for mobile devices. VGG16 is the model with the lowest network depth. Nevertheless, the increased network depth of a CNN model does not translate that the model has the ability to solve any problem. Moreover, as each problem typically involves distinctive features, all the CNN models may not exert the same effect on the same problem. In our study, VGG16, which has lower network depth compared to other CNN models, provided a more effective outcome for the problem compared to other models. Additionally, it should be recognized that the extent of the data used in the study was also effective on the analysis results.

The study evaluated the effectivity of the CNN models based on several parameters including Sen, Spe, NPV, FPR, FDR, Acc, and F1 Score, respectively, and revealed that VGG16 had the highest diagnostic performance. Moreover, VGG16 attained the highest F1 score (0.7421), which is calculated as the harmonic mean of parameters including specificity, sensitivity, precision, and sensitivity (recall), and also attained the highest Acc value (0.7603) which represents the overall accuracy of the classification (Table 2).

The calculation of ROC curve and AUC for each CNN model indicated that VGG16 had a higher AUC value (0.83 ± 0.05) compared to all other models, implicating that the features extracted via VGG16

Table 2
Results of SVM classification performed with the use of all channels (Sen: Sensitivity, Spe: Specificity, Acc: Accuracy, SD: Standard Deviation, NPV: Negative Predictive Value, FPR: False Positive Rate, FDR: False Discovery Rate).

Model	Kernel function	Sen	Spe	NPV	FPR	FDR	Acc	F_1 score	AUC ± SD
VGG16	Poly	**0.7222**	**0.7952**	**0.7579**	**0.2047**	**0.2367**	**0.7603**	**0.7421**	**0.83 ± 0.05**
VGG19	Rbf	0.5920	0.8206	0.6875	0.1793	0.2489	0.7114	0.6621	0.76 ± 0.04
ResNet	Poly	0.6996	0.7269	0.7258	0.2730	0.2991	0.7139	0.7002	0.78 ± 0.04
DenseNet	Rbf	0.5729	0.8380	0.6821	0.1619	0.2361	0.7114	0.6547	0.77 ± 0.05
MobileNet	Rbf	0.6180	0.6841	0.6620	0.3158	0.3586	0.6525	0.6295	0.70 ± 0.05
NasNetMobile	Poly	0.6423	0.6613	0.6693	0.3380	0.3654	0.6525	0.6384	0.72 ± 0.06
NasNetLarge	Rbf	0.3976	0.8095	0.5951	0.1905	0.3438	0.6127	0.4951	0.65 ± 0.05

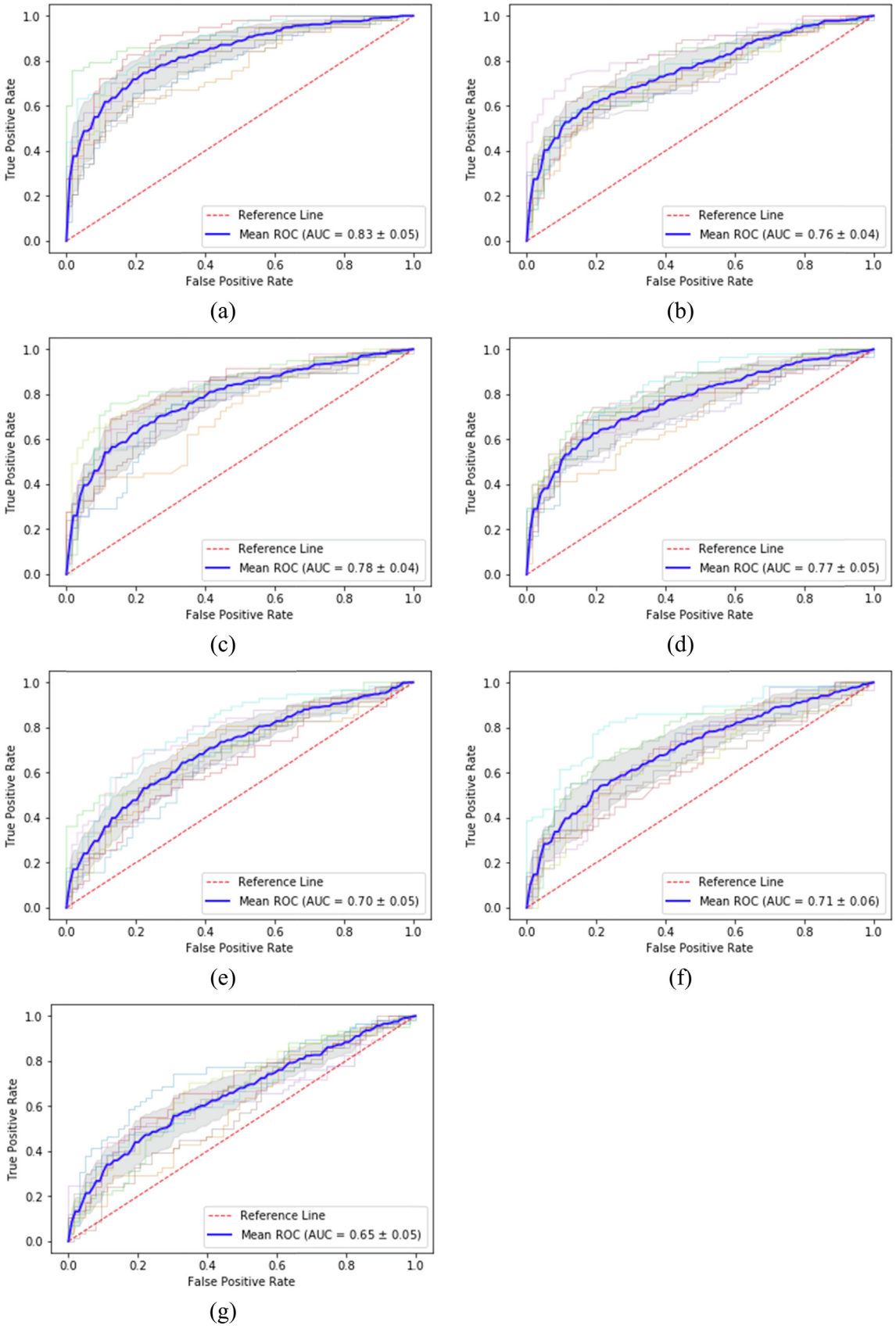

Fig. 6. ROC curves for each CNN model. (a) VGG16, (b) VGG19, (c) ResNet, (d) DenseNet, (e) MobileNet, (f) NasNetMobile, (g) NasNetLarge.

had a higher discriminatory ability compared to those of other CNN models (Fig. 6a).

Nevertheless, although this AUC value was close to 1, the value which indicates excellent discriminatory ability, it is not sufficient to confirm that this model is practically feasible. Nonetheless, the present study is a pioneer investigation into the determination of speech laterality via EEG signals and the classification results obtained in the study are promising and lead the way for subsequent studies though not practically feasible.

Conclusion

The present study aimed to determine speech laterality by using EEG signals with machine learning techniques. Although other techniques Wada testing and fMRI have been commonly used for the determination of speech laterality, both of them have been shown to have several disadvantages; Wada testing has been shown to be an invasive and difficult technique and fMRI has been reported to be a time-taking technique which is also difficult to access.

The present study is a pioneer investigation into the determination of speech laterality via EEG signals with machine-learning techniques, which, to our knowledge, has never been reported in the literature. These machine-learning techniques consisted of various CNN models, all of which were used for feature extraction and evaluated with regard to their performance in the classification of EEG signals. However, although the classification performance levels of the models were relatively higher than those reported in the literature, these levels were found to be inadequate to enable these models to be used in general practice. Nevertheless, considering that Wyllie et al. found that 5 out of 66 right-hand dominant subjects had right-hemisphere dominance and 3 out of 6 left-hand dominant subjects had left-hemisphere dominance, the overall accuracy level of ~80% attained by the CNN models used in the present study seems highly conceivable. Moreover, this limitation could be attributed to the paucity of data regarding the classification and evaluation of EEG signals and to the requirement of larger datasets for deep learning-based classifications.

The present study, as a pioneering investigation of the determination of speech laterality via EEG signals in lieu of time-taking procedures such as fMRI and invasive methods such as Wada testing, will provide significant support to neuroscientist in terms of the training of CNN models.

Future studies are recommended to:

- Substantiate our findings by evaluating larger datasets,
- Provide clearer results by evaluating individuals previously identified with right- or left-hemisphere speech dominance on Wada testing or fMRI, and
- Evaluate speech laterality in small healthcare centers once the results of the present study become feasible.

Compliance with Ethical standards

Conflict of interest

All authors read and approved the final manuscript. None of the authors had a conflict of interest.

Ethical approval

Ethics approval for the study protocol was obtained from the local area heath ethics committee.

Informed consent

Informed consent was obtained from all individual participants included in the study.

Appendix A. Supplementary data

Supplementary data to this article can be found online at https://doi.org/10.1016/j.mehy.2019.109315.

References

[1] Tailby C, Abbott DF, Jackson GD. The diminishing dominance of the dominant hemisphere: language fMRI in focal epilepsy. NeuroImage: Clinical 2017;14:141–50.
[2] White LE, Lucas G, Richards A, Purves D. Cerebral asymmetry and handedness. Nature 1994;368:197–8.
[3] Joliot M, Tzourio-Mazoyer N, Mazoyer B. Intra-hemispheric intrinsic connectivity asymmetry and its relationships with handedness and language Lateralization. Neuropsychologia 2016;93(Pt B):437–47.
[4] https://wiki.rit.edu/pages/viewpage.action?pageId=88966742 (Date Accessed: 09.06.2019).
[5] Tülay EE. "Beyin Elektriksel Aktivitesinin Ölçümü Ve Sinyal Analizi" Master Thesis İstanbul: Istanbul Kultur University- Fen Bilimleri Enstitüsü; 2009.
[6] Geschwind N, Galaburda AM. Cerebral lateralization biological mechanisms", Ass. and pathology. part I. A hypothesis and a program for research. Arch Neurol 1985;42(5):428–59.
[7] Peters L, Smedt BD. Arithmetic in the developing brain: a review of brain imaging studies. Dev Cognit Neurosci 2018;30:265–79.
[8] Knecht S, Dräger B, Deppe M, Bobe L, Lohmann H, Flöel A, et al. Handedness and hemispheric language dominance in healthy humans. Brain 2000;123(12):2512–8.
[9] Springer JA, Binder JR, Hammeke TA, Swanson SJ, Frost JA, Bellgowan PSF, et al. Language dominance in neurologically normal and epilepsy subjects: a functional MRI study. Brain 1999;122(11):2033–46.
[10] Binder JR, Swanson SJ, Hammeke TA, Morris GL, Mueller WM, Fischer M, Benbadis S, Frost JA, Rao SM, Haughton VM. Determination of language dominance using functional MRI: a comparison with the Wada test. Neurology 1996;46(4):978–84.
[11] Şengür A, Akılotu BN, Tuncer SA, Kadiroğlu Z, Yavuzkılıç S, Budak Ü, Deniz E. Optic disc determination in retinal images with deep features. Izmir: 2018 26th Signal Processing and Communications Applications Conference (SIU); 2018. p. 4–7.
[12] Lundervold AS, Lundervold A. An overview of deep learning in medical imaging focusing onMRI. Z Med Phys 2019;29(2):102–27.
[13] Jurcak V, Tsuzuki D, Dan I. 10/20, 10/10, and 10/5 systems revisited: Their validity as relative head-surface-based positioning systems. NeuroImage 2007;34(4):1600–11.
[14] Yuan L. Patients' EEG Data Analysis via Spectrogram Image with a Convolution Neural Network. Intelligent Decision Technologies (IDT 2017); 2017. p. 13–21.
[15] Keras Documentation. https://keras.io /applications. (Date Accessed: 02.04.2019).
[16] Krizhevsky A, Sutskever I, Hinton GE. ImageNet Classification with Deep Convolutional Neural Networks. Proceedings of the 25th International Conference on Neural Information Processing Systems; 2012. p. 1097–105.
[17] Gopalakrishnan K, Khaitan SK, Choudhary A, Agrawal AA. Deep Convolutional Neural Networks with transfer learning for computer vision-based data-driven pavement distress detection. Constr Build Mater 2017;157:320–30.
[18] Zagoruyko S, Komodakis N. Wide Residual Networks. arXiv:1605.07146v4 2017.
[19] Huang G, Liu Z, Maaten LVD, Weinberger KQ. Densely Connected Convolutional Networks. 2017 IEEE Conference on Computer Vision and Pattern Recognition (CVPR); 2017. p. 2261–9.
[20] Howard AG, Zhu M, Chen B, Kalenichenko D, Wang W, Weyand T, Andreetto M, Adam H. MobileNets: efficient convolutional neural networks for mobile vision applications. arXiv preprint arXiv:1704.04861 2017.
[21] Zoph B, Vasudevan V, Shlens J, Le QV. Learning transferable architectures for scalable image recognition. The IEEE Conference on Computer Vision and Pattern Recognition (CVPR); 2018.
[22] Khazaee A, Ebrahimzadeh A. Classification of electrocardiogram signals with support vector machines and genetic algorithms using power spectral features. Biomed Signal Process Control 2010;5(4):252–63.
[23] Tuncer SA, Alkan A. A decision support system for detection of the renal cell cancer in the kidney. Measurement 2018;123:298–303.
[24] Toraman S, Girgin M, Üstündağ B, Türkoğlu İ. Classication of the likelihood of colon cancer with machine learning techniques using FTIR signals obtained from plasma. Turk J Elec Eng Comp Sci 2019;27:1765–79.
[25] Tuncer SA, Akılotu B, Toraman S. A deep learning –based decision support system for diagnosis of OSAS using PTT signals. Medical Hypotheses 2019;127:15–22.
[26] Tomak L, Bek Y. İşlem Karakteristik Eğrisi Analizi ve Eğri Altında Kalan Alanların Karşılaştırılması. J Exp Clin Med 2010;27:58–65.
[27] Ng S, Susanna T Wilson, Tat-On C, Kin-Wang T, Ngai J, Chan KKP, et al. Use of Berlin questionnaire in comparison to polysomnography and home sleep study in patients with obstructive sleep apnea". Respir Res 2019;20(40).
[28] Wyllie E, Lüders H, Murphy D, Morris H, Dinner D, Lesser R, Godoy J, Kotagal P, Kanner A. Intracarotid amobarbital (wada) test for language dominance: correlation with results of cortical stimulation. Epilepsia 1990;31:156–61.
[29] Tuszynski MH, Petito CK. Ischemic thalamic aphasia with pathologic confirmation. Neurology 1975;38.
[30] Mohr JP, Watters WC, Duncan GW. Thalamic hemorrhage and aphasia. Brain Lang. 1975;2(3).
[31] Maeshima S, Osawa A. Thalamic lesions and aphasia or neglect. Curr. Neurol Neurosci Rep. 2018;18(39).